Zuse Institute Berlin

Takustr. 7
14195 Berlin
Germany

LUZIE HELFMANN[1], NATAŠA DJURDJEVAC CONRAD[2], ANA DJURDJEVAC, STEFANIE WINKELMANN[3], CHRISTOF SCHÜTTE

From interacting agents to density-based modeling with stochastic PDEs

[1] 0000-0002-8188-8288
[2] 0000-0001-8422-4930
[3] 0000-0002-0114-7819

ZIB Report 1921 (June 2019)

Zuse Institute Berlin
Takustr. 7
14195 Berlin
Germany

Telephone: +49 30-84185-0
Telefax: +49 30-84185-125

E-mail: bibliothek@zib.de
URL: http://www.zib.de

ZIB-Report (Print) ISSN 1438-0064
ZIB-Report (Internet) ISSN 2192-7782

From interacting agents to density-based modeling with stochastic PDEs

Luzie Helfmann[a,b,*], Nataša Djurdjevac Conrad[b], Ana Djurdjevac[c], Stefanie Winkelmann[b] and Christof Schütte[a,b]

[a]Freie Universität Berlin, Institut für Mathematik, Berlin, Germany
[b]Zuse Institute Berlin, Berlin, Germany
[c]Technische Universität Berlin, Institut für Mathematik, Berlin, Germany
[*]Corresponding author: luziehelfmann@gmail.com

June 11, 2019

Abstract

Many real-world processes can naturally be modeled as systems of interacting agents. However, the long-term simulation of such agent-based models is often intractable when the system becomes too large. In this paper, starting from a stochastic spatio-temporal agent-based model (ABM), we present a reduced model in terms of stochastic PDEs that describes the evolution of agent number densities for large populations. We discuss the algorithmic details of both approaches; regarding the SPDE model, we apply Finite Element discretization in space which not only ensures efficient simulation but also serves as a regularization of the SPDE. Illustrative examples for the spreading of an innovation among agents are given and used for comparing ABM and SPDE models.

Keywords Agent-based modeling, Model reduction, Dean-Kawasaki model, SPDEs, Finite Element method

1 Introduction

Modeling real-world dynamics is of great importance for the understanding, prediction and manipulation of the dynamical process of interest. Mathematically, one is therefore interested in the model analysis, inference of its parameters, as well as the accurate simulation and control of the dynamics. The modeling of realistic processes is nowadays often based on formulations in terms of discrete and autonomous entities (e.g. humans, institutions, companies), so-called agents, that move in a given environment and interact with each other according to a set of rules. Agent-based models (ABMs) are very flexible in their description, often they just consist of a set of behavioural rules for agents encoded in computer programs [5, 41]. Due to their versatility, ABMs are very attractive for modelers of various complex applications and disciplines (e.g. social sciences [2, 41], ecology [28, 27], archaeology [25, 24, 44]) and for including data into models. However, the different existing formulations of ABMs appear to be quite inconsistent and lack rigorous theoretical foundation, which motivates to develop standardized formats for these models [26, 2, 21].

In [7, 8], a mathematical formulation of an ABM is presented for systems of spatially distributed agents that move randomly in space and interact whenever they are close-by. The local interactions among agents trigger them to change their type, e.g. their opinion, or their infection status. The model is formulated as a system of equations coupling the diffusion dynamics for the spatial agent movement with Markov jump processes for the type changes of each agent. Agent-based models of

this class can for instance be found as models for infection spreading [6, 45], innovation spreading [7, 8] and chemical reactions [13].
In general, these ABMs cannot be solved analytically, but require numerical methods for simulating realizations of the modeled dynamics. In [7], a joint algorithm for the simulation of the spatial diffusion and the event-based interaction process is presented, building on the Euler-Maruyama scheme [31] and the Temporal Gillespie algorithm [49]. As the model formulation is stochastic, many Monte-Carlo (MC) simulations are required in order to make adequate predictions for observables of the system. However, for most real-world dynamics, such MC simulations are intractable due to an explosion of the costs for increasing agent numbers. Model reductions with a small approximation error are therefore necessary.

For spatial systems of many interacting agents, one can reduce the model complexity by replacing the micro-scale model of individual agents by a meso-scale model of stochastic agent densities, leading to a system of coupled stochastic partial differential equations (SPDEs) [11, 34, 4, 36]. Classically, in the limit of infinitely many agents, stochastic effects become negligible and the dynamics can be described by a macro-scale model of deterministic reaction-diffusion PDEs [46, 20]. In a real-world system, however, the number of agents is typically finite, such that the dynamics are still intrinsically random and stochastic modeling approaches are more appropriate e.g. in order to reflect the uncertainty and cover the emerging phenomena of the underlying ABM.

In this paper, after reviewing and slightly generalizing the stochastic ABM from [7, 8], we will formulate a system of SPDEs as a meso-scale approximation to the ABM, compare [30]. The model is an extension of the Dean-Kawasaki model [11, 34] that describes the transport in space of the stochastic agent densities and includes interactions between the agent densities for the different types [36, 4]. The derived distribution-valued equations belong to the class of Dean-Kawasaki type problems, for which well-posedness is still unresolved due to several mathematical difficulties [9, 38, 18]. Since in the end we are interested in the discretization of the model, we will, in order to deal with these issues, interpret the system of SPDEs in its weak form and consider "a regularization by discretization".
Henceforth, we propose an algorithm for the efficient sampling of trajectories of the coupled SPDE system by first discretizing in space using the Finite Element (FE) method, thereby approximating the unknown distributions by piece-wise polynomial functions. The resulting system of SDEs is well-posed and can be further discretized in time using the Euler-Maruyama method. As a meso-scale approach, simulation of the system of SPDEs is much faster than of the corresponding ABM, since the number of coupled equations is drastically reduced from scaling with the number of agents to scaling with the number of different agent types.
Last, we will study the ABM and the reduced SPDE model numerically on a toy example by comparing the computational effort and investigating the approximation quality of the reduced SPDE model with respect to the ABM.

2 Agent-based Model

Agent-based models are micro-scale computational models describing the system of interest in terms of discrete entities, called agents. An agent represents an autonomous entity such as a chemical particle, a person, a group of people or an organization. The individual behaviour of each agent is traced in space and time, including its interactions with other agents and the environment. The hope is that from the interplay of the local behaviour of agents on the microscopic scale, global patterns emerge on a larger system scale [29, 41, 28]. Emergence is likewise often stated as "the whole is more than the sum of its parts" due to the interactions among the parts (i.e. the agents) resulting in global structures [5].

In this section, we will review and slightly generalize the agent-based model from [7, 8], which is formulated as a system of stochastic processes describing the position dynamics and the interaction rules for agents. The position dynamics of agents are described by Brownian motion with a drift term pushing them towards suitable parts of their local surroundings. This is a useful description in the case that agents move randomly and slightly jittery in space whilst following some (hidden) energy landscape, e.g. when describing the mobility of humans in the ancient world [44], the movement of animals, or the diffusion of chemical particles [13].
Further, agents can interact according to a set of predefined rules whenever they are close in space. These interactions cause agents to change their type influenced by the state of other near-by agents (e.g. their infection status [35, 45], their current opinion [33], whether they use an innovation [8, 7], whether they have a certain information). The type changes are commonly written as $T_1 + T_3 \to T_2 + T_3$ (inspired by the notation for chemical reactions), where T_1, T_2, T_3 denote different agent types.
Even though the model formulation is very simple, it generates a vast range of different and complex outcomes on a larger system scale, e.g. exhibiting noise-induced tipping [8, 7, 47, 1].

The presented ABM is based on the Doi model [13] for reacting and locally diffusing chemical particles. It has similarities to the SIR model for infection spreading [35, 45] and to Brownian agents [48] and builds on the ABM for innovation spreading in the ancient world as introduced in [8, 7].

We will give a detailed description of the agent-based model in Section 2.1, and explain a method for its simulation in Section 2.2.

2.1 Model Formulation

We consider a system of N agents, where each agent $i = 1, \dots, N$ is characterized by its type $Y_i(t)$ and its position $X_i(t)$ at time $t \in [0, T]$. The agents' positions can be continuous values in a given domain $D \subseteq \mathbb{R}^d$, whereas the type of an agent is a discrete feature denoted by values in $\{1, \dots, N_T\}$. Thus the state of the i^{th} agent at time t is given by $(X_i(t),\ Y_i(t)) \in D \times \{1, \dots, N_T\}$. We write the state of the whole system of N agents as $(X(t), Y(t)) = (X_i(t),\ Y_i(t))_{i=1}^N$.

In the model, we are following every agent $i = 1, \dots, N$ individually and track the evolution in time of its position state and type. The position dynamics and the interactions between agents leading to type changes are described in the following sections.

2.1.1 Position Dynamics of Agents

We assume that agents are able to move and change their position in the domain $D \subseteq \mathbb{R}^d$. Thereby agents are taking their local surroundings into account, in such a way, that they are attracted to near-by regions that are suitable for them and refrain from unsuitable parts of the domain.
We can straightforwardly model this by letting the agents follow the gradient of a potential landscape, the so-called suitability landscape. The suitability landscape V indicates the attractivity of the environment and gives an incentive for agents to prefer or avoid certain near-by parts of the domain. Valleys of the suitability landscape correspond to attractive regions and peaks and divides correspond to unsuitable areas that are moreover difficult to overcome. The suitability landscape can be constructed on the basis of data and expert knowledge, see e.g. [7, 8, 44].
Additionally, we include randomness in the agents' motion to account for other unknown incentives for positional changes and to allow agents to be exploratory or make mistakes in their evaluation of the environment.

Thus, the change of the position $X_i(t) \in D \subseteq \mathbb{R}^d$ of every agent $i = 1, \dots, N$ is governed by the

Itô diffusion process

$$dX_i(t) = -\nabla V(X_i(t))dt + \sigma dB_i(t), \tag{1}$$

with gradient operator $\nabla = \left(\frac{\partial}{\partial x_1}, \ldots, \frac{\partial}{\partial x_d}\right)^T$, suitability landscape $V : D \subseteq \mathbb{R}^d \to \mathbb{R}$, diffusion constant $\sigma \in \mathbb{R}$ and $B_i(t)$ denoting independent standard Brownian motions in $\mathbb{R}^d$. We impose reflecting boundary conditions in the case where D is bounded and thereby ensure that the agents' positions are within D for all times.

Remark. The position dynamics of agents in many modeling scenarios are interdependent such that agents tend to group together in space and form clusters, while also keeping some distance from each other in order to avoid spatial overlap and crowding [8, 7]. To account for this, another drift term has to be added to the position SDE (1), s.t. the dynamics are governed by

$$dX_i(t) = -\left(\nabla V(X_i(t)) + \nabla U_i(X(t))\right) dt + \sigma dB_i(t). \tag{2}$$

Thereby each agent i experiences an additional force derived from the attraction-repulsion potential U_i

$$U_i : D^N \subseteq \mathbb{R}^{d\times N} \to \mathbb{R},\ X(t) \mapsto \sum_{j\neq i} u\left(\|X_i(t) - X_j(t)\|\right), \tag{3}$$

where we sum over all pair-wise attraction-repulsion potentials $u : \mathbb{R}_{\geq 0} \to \mathbb{R}$ between agent i and $j \neq i$. The pair-wise potentials u are inspired by interatomic potentials from Physics (e.g. Lennard-Jones potential, Buckingham potential). Attraction between pairs of agents occurs whenever agents at long distances are driven towards another, and repulsion appears when agents are forced apart at short distances. Agents are thus searching for an optimal balance between forming clusters of agents on the one hand and distributing in space on the other hand.

2.1.2 Interaction Rules

Agents can change their type according to a set of N_R interaction rules $\{R_r\}$, $r = 1, \ldots, N_R$. The type changes happen at a certain rate and whenever an agent is in proximity of specific other agents that can influence the agents' type. We consider rules $\{R_r\}$ that can be written as the type change[1]

$$R_r :\ T_s + T_{s''} \to T_{s'} + T_{s''} \text{ with } s, s', s'' \in \{1, \ldots, N_T\} \tag{4}$$

happening at the fixed influence rate γ^r_{ABM} and triggered by a close-by agent of type $T_{s''}$.

For example when modeling the spreading of an innovation among humans [7, 8], we can assume that every agent takes one of the two discrete innovation states: T_1 for a non-adopter or T_2 for an adopter of the innovation. By defining one simple interaction rule R_1: $T_1 + T_2 \to 2\ T_2$, we can model that adopters pass on the innovation to non-adopters at a fixed rate whenever they are in contact.

Pairs of agents are in contact if they are within a distance d_{int} of each other. Given the changing positions of agents (1), we construct a time-evolving network between agents (represented by the set of nodes) that are in contact (given by the edges) at time t. The network is fully determined by a time-dependent adjacency matrix $\mathcal{A}(t) = (\mathcal{A}_{ij}(t))_{i,j=1}^N$ with entries $\mathcal{A}_{ij}(t) = 1$ if $i \neq j$, $\|X_i(t) - X_j(t)\| \leq d_{\text{int}}$, and 0 else.

As a next step, we are interested in describing the type change process $\{Y_i(t)\}_{t\in[0,T]}$ of each agent i. If agent i at time t is of type T_s, $s \in \{1, \ldots, N_T\}$, we denote this by $Y_i(t) = s$. Type changes

[1] In principle, the interaction rules could be of a more complicated form, e.g. by including the death and birth of agents such as $T_s \to \varnothing$ and $T_s + T_{s''} \to T_{s'}$ or by allowing both agents to change their type $T_s + T_{s''} \to T_{s'} + T_{s'''}$.

for agent i are modeled as Markov jump processes on $\{1, \dots, N_T\}$ with time-dependent transition rates. The transition rates are changing in time since they depend both on the proximity of other agents and their types. The transition rate function $\lambda_i^r(t)$ gives the accumulated rate for agent i of type T_s to change its type according to interaction rule R_r and is proportional to the constant influence rate γ_{ABM}^r and to the number of neighbors of agent i that trigger interaction R_r, i.e. the number of agents of type $T_{s''}$ in rule (4).
Consequently, we write the transition rate function for agent i at time t following interaction rule $R_r: \; T_s + T_{s''} \to T_{s'} + T_{s''}$ as

$$\lambda_i^r(t) = \lambda_i^r(\mathcal{A}(t), Y(t)) = \gamma_{\text{ABM}}^r \sum_{j=1}^{N} \mathcal{A}_{ij}(t) \; \mathbb{1}_{\{s''\}}(Y_j(t)) \; \mathbb{1}_{\{s\}}(Y_i(t)), \tag{5}$$

where $\mathbb{1}_B$ is the indicator function defined as $\mathbb{1}_B(x) = 1$ if $x \in B$ and 0 else.

Finally, the type change process $\{Y_i(t)\}_{t\in[0,T]}$ of agent i can be expressed as

$$Y_i(t) = Y_i(0) + \sum_{r=1}^{N_R} \mathcal{P}_i^r \left(\int_0^t \lambda_i^r(t')dt' \right) v_r, \tag{6}$$

where $Y_i(0)$ denotes the initial type of agent i, $\mathcal{P}_i^r$ denote i.i.d. unit-rate Poisson processes and the type change vector is denoted by $v = (v_r)_{r=1}^{N_R}$ ($v_r = s' - s$ for R_r as given in (4) above).

2.1.3 Formulation of the Agent System Dynamics

Putting together Equations (1) and (6), we can describe the evolution in time of the agent states by the following coupled equations

$$\begin{aligned} X_i(t) &= X_i(0) - \int_0^t \nabla V(X_i(t'))dt' + \sigma \int_0^t dB_i(t') \\ Y_i(t) &= Y_i(0) + \sum_{r=1}^{N_R} \mathcal{P}_i^r \left(\int_0^t \lambda_i^r(t')dt' \right) v_r \end{aligned} \tag{7}$$

for agents $i = 1, \dots, N$.

Since we cannot solve the coupled equations (7) analytically, we will in the following explain how to accurately discretize and efficiently simulate trajectories of the dynamics.

2.2 Simulation

For each agent i, the type change process depends on the positions and on the types of all other agents via the time-dependent transition rate functions $\lambda_i^r(t)$. If we additionally include attraction-repulsion forces between agents, then further the motion of all agents is intrinsically intertwined. For the design of the simulation algorithm we have to take this into account and therefore propose to simulate both the position and type changes (7) in parallel.

The most straightforward approach is to discretize time $[0, T]$ with sufficiently small Δt time steps. The Euler-Maruyama method can be employed to accurately and efficiently discretize the SDE [37, 7], whereas when discretizing the Markov jump processes we replace rates by probabilities in each time step [8, 7]. The resulting simulation approach can be summarized as follows.

For each time step $t_k = k\Delta t$, $k = 0, \dots, K-1$:

1. For each agent $i = 1, \dots, N$: the positions are advanced according to

$$X_i(t_{k+1}) = X_i(t_k) - \nabla V(X_i(t_k))\Delta t + \sigma\sqrt{\Delta t} \; \zeta_{i,k}$$

with i.i.d. $\zeta_{i,k} \sim \mathcal{N}(0, 1)$.

2. For each $i = 1, \dots, N$, $r = 1, \dots, N_R$: agent i changes its type according to rule R_r with probability

$$p_i^r(t_k) = 1 - \exp(-\lambda_i^r(t_k)\Delta t).$$

We could simulate the type changes more accurately [19] by simulating them continuously in time using a stochastic simulation algorithm [49], for the simulation approach in this case we refer the reader to [7].

In addition to the fact that the algorithm scales linearly with the number of agents N, there are some hidden costs. In each time step, we need to compute the contact network $\mathcal{A}(t_k)$, i.e. the pair-wise distances between agents. The brute-force approach of computing all pair-wise distances scales like $\mathcal{O}(N^2)$ for N agents. These distances are also required when including attraction-repulsion forces, since the pair-wise attraction-repulsion potential $u(\|X_i(t) - X_j(t)\|)$ depends on the pair-wise distances between agents.

The proposed simulation algorithm produces a single trajectory of the joint stochastic process $\{X(t), Y(t)\}_{t\in[0,T]}$. In order to obtain reliable statistics of the dynamics and to estimate the process' distribution and its moments, several thousand repeated simulations are required. In case of a system with large numbers of agents this causes problems since the simulation cost scales badly with increasing agent numbers N. Parameter studies are numerically not tractable in this case. Many real-world systems actually contain very large numbers of agents, which motivates to consider a less complex modeling approach in terms of stochastic PDEs, and thereby offers a cheap method for simulating trajectories.

3 Model Reduction to a System of Stochastic PDEs

Instead of studying the evolution of every individual agent, in the following we study the transport in space and the interactions between agents in terms of number densities for each type, such that the model complexity and simulation costs are drastically reduced. This reduced model, given in the form of a system of stochastic PDEs, is a combination of the model for position changes proposed by Dean and Kawasaki [11, 34] (also termed Dean-Kawasaki model), and added terms for the interactions between agent densities [4, 36]. It approximates the ABM for systems of many, but finitely many agents. Stochasticity still emerges from the systems' inherent randomness due to the finite number of agents. But agents become indistinguishable among their type and we lose the individual agent labels, see Figure 1.

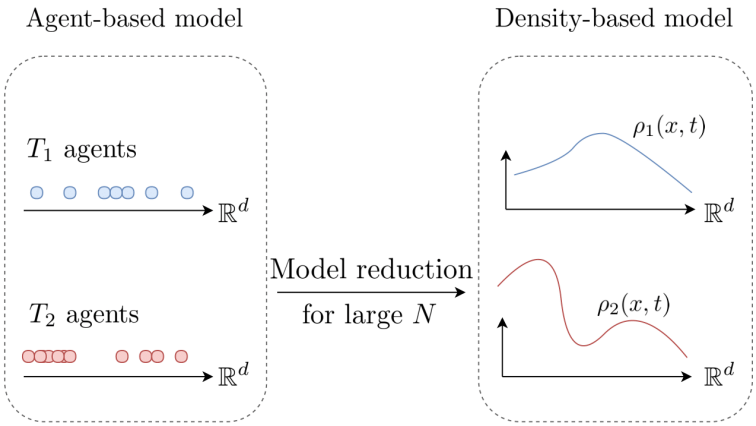

Figure 1: Model reduction from the agent-based formulation in terms of N discrete agents to the SPDE description in terms of agent number densities $\rho_s(x,t)$ for types $s = 1, \dots, N_T$.

Applications of similar SPDE models include chemical pattern formation [4, 36] and models for bacterial populations [23], but to our knowledge they have not yet been applied for modeling systems of humans.

We will start by proposing and explaining the features of the reduced SPDE model in Section 3.1. In Section 3.2, we will tackle its efficient numerical discretization by means of the Finite Element method.

3.1 Model Formulation

We are considering a model describing the stochastic evolution of agent number densities (or number concentrations) for each agent type $s = 1, \dots, N_T$. The (stochastic) agent number density

$$\rho_s : D \times [0,T] \mapsto \mathbb{R}_{\geq 0},$$

is defined on the domain $D \subseteq \mathbb{R}^d$, the time interval $[0,T]$ and with probability space $(\Omega, \mathcal{F}, \mathbb{P})$[2]. Integrating the number density ρ_s over the domain yields the number of agents of type T_s, which we denote by N_s.

The densities $(\rho_1(x,t), \dots, \rho_{N_T}(x,t))$ evolve due to diffusion and drift in the suitability landscape and because of the set of interaction rules. The temporal changes of $\rho_s(x,t)$ for $s = 1, \dots, N_T$ are given by the following stochastic partial differential equation (SPDE) interpreted in the Itô sense

$$\frac{\partial \rho_s(x,t)}{\partial t} = \mathcal{D}\rho_s(x,t) + \mathcal{I}\rho_s(x,t) \tag{8}$$

with stochastic diffusion operator $\mathcal{D}$ (see Section 3.1.1) and stochastic interaction operator $\mathcal{I}$ (Section 3.1.2). For a fixed sample $\omega \in \Omega$, the agent density is a realization of a stochastic process solving the SPDE.

3.1.1 Diffusion of the Agent Densities

The diffusion operator in Equation (8) is given by [11, 34, 36, 4]

$$\mathcal{D}\rho_s(x,t) := \frac{\sigma^2}{2}\Delta\rho_s(x,t) + \nabla \cdot (\nabla V(x)\rho_s(x,t)) + \sigma\nabla \cdot \left(\sqrt{\rho_s(x,t)} Z_s^{\mathcal{D}}(x,t)\right) \tag{9}$$

with diffusion constant $\sigma \in \mathbb{R}$, Laplace operator $\Delta = \sum_{l=1}^{d} \frac{\partial^2}{\partial x_l^2}$ and suitability landscape $V : D \subseteq \mathbb{R}^d \mapsto \mathbb{R}$. $Z_s^{\mathcal{D}}(x,t) = \left(Z_{s,1}^{\mathcal{D}}(x,t), \dots, Z_{s,d}^{\mathcal{D}}(x,t)\right)$ denotes a d-dimensional vector of space-time white noise (STWN) for the diffusion, i.e. a mean zero process that is uncorrelated in space and time

$$\mathbb{E}\left(Z_{s,j}^{\mathcal{D}}(x,t) Z_{s',j'}^{\mathcal{D}}(x',t')\right) = \delta_{jj'}\delta_{ss'}\delta(x-x')\delta(t-t'),$$

where δ_{ij} denotes the Kronecker Delta and $\delta(x-y)$ denotes the Dirac Delta distribution. The diffusive part of the SPDE evolves a number density of many agents and is responsible for the diffusive transport in space with drift in the suitability landscape $V(x)$. Its deterministic part $\partial_t \rho_s = \frac{\sigma^2}{2}\Delta\rho_s + \nabla \cdot (\nabla V \rho_s)$ reminds of the Fokker-Planck equation that describes the evolution of a density of infinitely many non-interacting particles that are diffusing with drift in a potential.
In our case, we consider a large but finite number of diffusing particles, as such the system is still intrinsically random and the derivation leads to an additional noise term fluctuating around zero.

[2] Actually the number density should be $\rho_s(\omega, x, t)$ but we do not write the explicit dependence on $\omega \in \Omega$. The agent number density is random since it solves a stochastic PDE.

The derivation [11, 34] of $\frac{\partial \rho_s}{\partial t} = \mathcal{D}\rho_s$ from the position SDE (1) is based on the following idea: We define the empirical agent density for a single agent i as

$$\rho^i(x,t) = \delta(x - X_i(t)), \tag{10}$$

where $\delta(x - X_i(t))$ denotes a Dirac Delta distribution placed at position $X_i(t)$. Then, using Itô's Formula, the SDE (1) for agent i is transformed into an SPDE describing the temporal evolution of $\rho^i(x,t)$. We sum the SPDEs over $i = 1, \dots, N_s$ to get an equation for the density of all agents of type T_s, i.e. for $\rho_s(x,t) = \sum_{i=1}^{N_s} \rho^i(x,t)$. Aiming at a closed-form equation for $\rho_s(x,t)$, we then replace the noise term by a different noise term of the same mean and covariance that just depends on $\rho_s(x,t)$.

This multiplicative noise term $\sigma \nabla \cdot (\sqrt{\rho_s} Z_s^{\mathcal{D}})$ is non-linear and comes with several mathematical problems, making the question of existence and uniqueness of the solution still an open problem [9, 38]. First, the noise term is given in a divergence form. In order to interpret this term, we will consider the weak formulation and use partial integration to transfer the divergence operator to the test functions. Second, the meaning of the term $\sqrt{\rho_s}$ remains undefined. Namely, the unknown ρ_s is defined as a sum of Dirac Delta distributions, hence the meaning of its square root is unclear. We will deal with this problem by approximating the distribution ρ_s by a function from a Finite Element space, for which the square root is well defined.
Different notions of solutions to (9) that would be natural to consider exist, such as a martingale solution [38] or a path-wise kinetic solution [18]. In order to apply the Finite Element method and to reformulate the divergence of the noise term, in our setting it is more appropriate to consider the weak formulation (in the PDE sense) that will be derived in 3.1.4.

Remark. We can extend the diffusion operator to include attraction forces between pairs of agents at long ranges and repulsion forces at short ranges, similar as in Equation (2). Denoting the pairwise attraction-repulsion potential between two agents at positions x and y by $u(\|x-y\|)$, the SPDE is extended by one term (the derivation can be found in [11])

$$\mathcal{D}\rho_s(x,t) = \frac{\sigma^2}{2}\Delta\rho_s(x,t) + \nabla \cdot (\nabla V(x)\rho_s(x,t)) + \nabla \cdot \left(\rho_s(x,t) \int_D \left(\sum_{s'=1}^{N_T} \rho_{s'}(y,t)\right) \nabla u(\|x-y\|) dy\right)$$
$$+ \sigma \nabla \cdot \left(\sqrt{\rho_s(x,t)} Z_s^{\mathcal{D}}(x,t)\right). \tag{11}$$

The additional term models the diffusion of the agent density $\rho_s(x,t)$ in the aggregated attraction-repulsion potential of the density of all agents $\sum_{s'} \rho_{s'}(x,t)$. Including this term, the diffusing densities are all coupled to each other.
For analytical simplicity, we won't further consider attraction and repulsion forces in the remaining paper. But it should be possible to extend the discretization of the SPDE straightforwardly.

3.1.2 Interactions between Agent Densities

The interaction operator of the system of SPDEs (8) accounts for the local transport of some density between the different agent densities $\rho_s(x,t)$, $s = 1, \dots, N_T$ according to the set of interaction rules R_r, $r = 1, \dots, N_R$ [36, 4]

$$\mathcal{I}\rho_s(x,t) := \sum_{r=1}^{N_R} \nu_s^r \left(a^r(\rho(x,t)) + \sqrt{a^r(\rho(x,t))} Z_r^{\mathcal{I}}(x,t)\right). \tag{12}$$

The coefficient ν_s^r describes the discrete number change of the type T_s agents involved in the r^{th} interaction rule[3], $a^r(\rho(x,t))$ is the transition rate function for densities according to rule R_r.

[3] In the chemistry literature, ν_s^r is called the stoichiometric coefficient of type T_s due to the r^{th} reaction. Further, for rules R_r of the form (4), ν_s^r and v_r (the type change coefficient from the ABM) are related via $v_r = \sum_s \nu_s^r s$.

Similar as in the ABM, the rate function depends on the local amount of the two types of agents taking part in the interaction. The more agents of each of the two types, the more interactions are happening. Also for a larger constant influence rate γ^r_{SPDE} (units of γ^r_{SPDE} are volume × inverse time), more interactions are happening per time. Thus for interaction rule $R_r : T_s + T_{s''} \to T_{s'} + T_{s''}$ with $s, s', s'' \in \{1, \dots, N_T\}$, the transition rate function at time t reads

$$a^r(\rho(x,t)) = \gamma^r_{\mathrm{SPDE}}\ \rho_s(x,t)\rho_{s''}(x,t). \tag{13}$$

To get a better understanding of these coefficients and functions, let us return to our innovation spreading example: agents of type T_1 and T_2 are interacting according to the rule $R_1 : T_1 + T_2 \to 2\,T_2$. Since for each interaction the number of type T_1 agents decreases by one agent and the number of type T_2 agents increases by one agent, we have $\nu^1_1 = -1,\ \nu^1_2 = 1$. The transition rate function for the interaction between two agent densities is proportional to the density of each and the meso-scale rate γ^1_{SPDE} such that $a^1(\rho(x,t)) = \gamma^1_{\mathrm{SPDE}}\ \rho_1(x,t)\rho_2(x,t)$ in this example.
Space-time white noise for the r^{th} interaction is denoted by $Z^{\mathcal{I}}_r(x,t)$ with covariance

$$\mathbb{E}\left(Z^{\mathcal{I}}_r(x,t)Z^{\mathcal{I}}_{r'}(x',t')\right) = \delta_{rr'}\delta(x-x')\delta(t-t').$$

In order to derive the interaction operator of the SPDE (12), the Poisson random variable for interactions in the agent-based description (6) has been replaced by a Gaussian random variable with the same mean and variance [36]. Further, the interaction parameters d_{int} and γ^r_{ABM} are aggregated to the meso-scale influence rate γ^r_{SPDE} [15, 17]. This approximation is only valid for large $a^r(\rho(x,t))$, and is closely related to the approximation that has been done for well-mixed systems of interacting species leading to the Chemical Langevin equation (CLE) [22] in the context of the so-called large population limit. Equation (12) includes spatial information and can be viewed as a spatial extension of the CLE.

Remark. In [36], in the context of numerical simulation of the model, the Gaussian noise is again replaced by Poisson noise in each grid cell. The reason for this is that the Gaussian approximation is only valid in the large population limit, i.e., for large numbers of agents in each grid cell. Switching back to Poisson noise helps decreasing the resulting lack of accuracy and preventing negative values for densities in numerical simulations; however, the procedure is rather ad-hoc and no precise understanding of its effect is available.

3.1.3 Complete Dynamics

For the system of SPDEs to be fully determined, boundary and initial conditions have to be specified. The domain boundary should be Lipschitz continuous. Since in our model agents cannot leave the domain, we require no-flux boundary conditions on δD. The initial data $\rho_{s,0}(x)$ has to be non-negative and such that $\int_D \rho_{s,0}(x)dx = N_s$. Then, for agent types $s = 1, \dots, N_T$ the system of SPDEs reads

$$\begin{aligned}
\frac{\partial \rho_s(x,t)}{\partial t} &= \mathcal{D}\rho_s(x,t) + \mathcal{I}\rho_s(x,t) && \text{on } D \times [0,T] \\
\nabla \rho_s(x,t) \cdot \hat{u}(x) &= 0 && \text{on } \delta D \times [0,T] \\
\rho_s(x,0) &= \rho_{s,0}(x) && \text{on } D \times \{0\}.
\end{aligned} \tag{14}$$

As we have now described the system of SPDEs, there are some further points worth noting. We can observe that the diffusion operator $\mathcal{D}$ (9) conserves the number of agents of each type because of the divergence operator form and assuming no-flux boundary conditions. It is solely responsible for the transport of the density in space. The interaction part (12) of the SPDE shifts the agent number density locally between the different agent types, but conserves the overall number

of agents of all types, i.e. $\sum_{s=1}^{N_T} \int_D \rho_s(x,t)dx = N$ is conserved since $\sum_s \nu_s^r = 0$ for each interaction rule of the form (4). In the case of more complicated interaction rules (e.g. the birth and death of agents), this is usually not the case.

We can also have a closer look at how the random forcings scale for increasing agent numbers, i.e. larger values of the density $\rho_s(x,t)$. The noise terms are scaled by a square-root factor of the agent density, whereas all the other (deterministic) terms are scaled by the density. Thus for the number of agents approaching zero, the noise dominates the SPDE. For the number of agents going to infinity, the noise terms become unimportant and could be neglected. Then, the SPDE could be replaced by a PDE model. Our numerical examples in Section 4 will display this behaviour.

The analysis of the well-posedness and existence of solutions to this SPDE system is not investigated enough [18, 38, 9]. In this paper though, we are concerned with a discretization of the SPDE system. We will in the following show how to formally derive the weak formulation of the system of SPDEs (Section 3.1.4) forming the basis for discretizing the SPDEs with the Finite Element method (Section 3.2).

3.1.4 Weak Formulation

The SPDE (14) is properly interpreted as an integral equation in time. For this, we will introduce the Cylindrical Wiener process $\{W(\cdot,t)\}_{t\in[0,T]}$ [40, 10] as

$$W(x,t) = \sum_{m=1}^{\infty} \chi_m(x) B_m(t), \tag{15}$$

where $\{\chi_m(x)\}_{m\in\mathbb{N}}$ is any orthonormal basis of $L^2(D)$ and $B_m(t)$ are i.i.d. Brownian motions in $\mathbb{R}$. The Cylindrical Wiener process is a stochastic process that is Brownian in time and white (i.e. uncorrelated) in space, such that its time derivative turns out to be space-time white noise $Z(x,t) = \partial_t W(x,t)$. By introducing the Cylindrical Wiener process expansion (15) into the SPDE (14), we can use the integral theory for stochastic processes in space and time [40, 10]. Additionally, this offers a straightforward possibility for simulating realizations of $Z(x,t)$ by truncating the expansion (15) to a finite number of terms, numerically differentiating in time, and sampling i.i.d. Brownian motions $B_m(t)$.

In order to find solutions of the system of SPDEs, we will consider the weak solution framework (in the PDE sense). For the derivation of the weak form, we interpret (14) with the introduction of (15) in the time integral sense, multiply it by test functions $w(x)$, integrate over the domain D, and use partial integration. As usual, by making use of partial integration in deriving the weak form, we reduce the regularity requirements of the solution $\rho_s(x,t)$. Moreover, utilizing the no-flux boundary conditions $\nabla\rho_s(x,t)\cdot\hat{u}(x) = 0$ on δD, we get

$$\langle \Delta\rho_s(\cdot,t), w\rangle = -\int_D \nabla\rho_s(x,t)\cdot\nabla w(x)\ dx + \int_{\delta D} (\nabla\rho_s(x,t)\cdot\hat{u}(x)) w(x)\ dx = -\langle \nabla\rho_s(\cdot,t), \nabla w\rangle.$$

Here and in the following, we use the inner product notation $\langle u,v\rangle = \int_D u(x)v(x)\ dx$.
Further, we shift the divergence operator from the space-time white noise onto the test functions. By using partial integration, we find

$$\left\langle \nabla\cdot\left(\sqrt{\rho_s(\cdot,t)}dW_s^{\mathcal{D}}(\cdot,t)\right), w\right\rangle = -\left\langle \sqrt{\rho_s(\cdot,t)}dW_s^{\mathcal{D}}(\cdot,t), \nabla w\right\rangle + \int_{\delta D}\left(\sqrt{\rho_s(x,t)}dW_s^{\mathcal{D}}(x,t)\cdot\hat{u}(x)\right) w(x)\ dx.$$

With that, the weak formulation of (14) consists of finding $\rho_s(x,t)$ for all agent types $s = 1,\dots,N_T$, such that

$$\begin{aligned}
\langle \rho_s(\cdot,t), w\rangle &= \langle \rho_{s,0}, w\rangle + \int_0^t \left(-\frac{\sigma^2}{2}\left\langle \nabla\rho_s(\cdot,t'), \nabla w\right\rangle + \left\langle \nabla\cdot\left(\nabla V \rho_s(\cdot,t')\right), w\right\rangle \right) dt' \\
&+ \sum_{r=1}^{N_R} \nu_s^r \int_0^t \left\langle a^r(\rho(\cdot,t')), w\right\rangle dt' - \sigma \int_0^t \left\langle \sqrt{\rho_s(\cdot,t')} dW_s^{\mathcal{D}}(\cdot,t'), \nabla w\right\rangle \\
&+ \sigma \int_0^t \left(\int_{\delta D} \left(\sqrt{\rho_s(x,t')} dW_s^{\mathcal{D}}(x,t')\cdot \hat{u}(x)\right) w(x)\, dx\right) + \sum_{r=1}^{N_R} \nu_s^r \int_0^t \left\langle \sqrt{a^r(\rho(\cdot,t'))} dW_r^{\mathcal{I}}(\cdot,t'), w\right\rangle \quad (16)
\end{aligned}$$

holds for all $w(x)$ and for all $t \in [0,T]$.
The integrals with respect to the Cylindrical Wiener process have to be understood as follows

$$\int_0^t \left\langle \sqrt{\rho_s(\cdot,t')} dW_s^{\mathcal{D}}(\cdot,t'), \nabla w\right\rangle = \sum_{l=1}^{d}\sum_{m=1}^{\infty} \int_0^t \left\langle \sqrt{\rho_s(\cdot,t')}\chi_m, \frac{\partial w}{\partial x_l}\right\rangle dB_{s,m,l}^{\mathcal{D}}(t')$$

$$\int_0^t \int_{\delta D} \left(\sqrt{\rho_s(x,t')} dW_s^{\mathcal{D}}(x,t')\cdot \hat{u}(x)\right) w(x)\, dx = \sum_{l=1}^{d}\sum_{m=1}^{\infty} \int_0^t \left(\int_{\delta D} \sqrt{\rho_s(x,t')}\chi_m(x)\hat{u}_l(x) w(x) dx\right) dB_{s,m,l}^{\mathcal{D}}(t')$$

$$\int_0^t \left\langle \sqrt{a^r(\rho(\cdot,t'))} dW_r^{\mathcal{I}}(\cdot,t'), w\right\rangle = \sum_{m=1}^{\infty} \int_0^t \left\langle a^r(\rho(\cdot,t'))\chi_m, w\right\rangle dB_{r,m}^{\mathcal{I}}(t').$$

This formal derivation of the weak form (16) is the foundation for discretizing the system of SPDEs in the following section.

3.2 Discretization of the System of SPDEs

Previously, we introduced a model (14) for the evolution of stochastic agent densities $\rho_s : D\times[0,T] \to \mathbb{R}_{\geq 0}$ that are being transported in space and interacting with each other. The existence and uniqueness of solutions to the SPDE are still an open question, especially in the last few years much research has been focused on this [18, 38, 9].
Here we instead propose a Finite Element discretization of the weak formulation of the system of SPDEs (16) via a finite spatial ansatz space and truncation of the noise expansion. The result of this Galerkin discretization will be the (finite) system of SDEs (28). For such SDEs rigorous statements concerning the existence and uniqueness of solutions exist: if the drift and noise intensity terms satisfy appropriate conditions regarding Lipschitz continuity and growth at infinity, then the solution exists and is unique [42, Chapter 2] and moreover stable with respect to perturbations of drift and noise intensity [42, Chapter 4].
The resulting system of SDEs can be further discretized in time, s.t. we arrive at (a sequence of) matrix equations that have to be solved at each time step.

The general steps of the spatial discretization are as follows [40]:

1. We project the solutions onto the finite-dimensional space $\tilde{V}$ (Section 3.2.1).
2. We truncate the expansion of the Cylindrical Wiener process $W^M(x,t) = \sum_{m=1}^{M} \chi_m(x) B_m(t)$ to M terms (Section 3.2.2).

In order to arrive at a fully discrete system we will perform a third step at last:

3. We discretize in time using the Euler-Maruyama scheme (Section 3.2.3).

The discretization of the system of SPDEs will allow us to very efficiently simulate trajectories that approximate the dynamics of the agent-based model.
Instead of discretizing the SPDE model with a Finite Element approach, one can also employ the Finite Volume method [36, 14, 12]. Here, we use the Finite Element method since it has the advantage that one can in principle treat very complicated domains which is needed for many real-world models. Further, due to the weak form interpretation, we can make sense of the divergence operator acting on the space-time white noise.

3.2.1 Space Discretization

We consider a simplicial discretization (e.g. by triangles, rectangles) $\tilde{D} = \tilde{D}(h)$ of the (possibly curvilinear) computational domain $D \subseteq \mathbb{R}^d$. Here h is defined as $h := \max_{E\in\mathcal{T}} h_E$, where h_E is the diameter of the simplex E and $\mathcal{T}$ is the union of all simplices. We let $\tilde{V} = \tilde{V}(h)$ be a finite-dimensional element space consisting of continuous piece-wise linear functions defined on $\tilde{D}$ and spanned by its nodal basis (e.g. hat functions) $\{\phi_i : \tilde{D} \to \mathbb{R}\}_{i=0}^n$. In the following, the inner product on the discretized domain $\tilde{D}$ is given by $\langle u, v\rangle_h = \int_{\tilde{D}} u(x)v(x)\, dx$.
The Finite Element method then reduces the problem (16) to finding $\tilde{\rho}_s(\cdot, t) \in \tilde{V}$ for each agent type $s = 1, \dots, N_T$ such that

$$\begin{aligned}
&\langle \tilde{\rho}_s(\cdot,t), \phi_i\rangle_h = \langle \tilde{\rho}_{s,0}, \phi_i\rangle_h + \int_0^t \left(-\frac{\sigma^2}{2} \left\langle \nabla\tilde{\rho}_s(\cdot,t'), \nabla\phi_i \right\rangle_h + \left\langle \nabla\cdot\left(\nabla V \tilde{\rho}_s(\cdot,t')\right), \phi_i \right\rangle_h \right) dt' \\
&+ \sum_{r=1}^{N_R} \nu_s^r \int_0^t \left\langle a^r(\tilde{\rho}(\cdot,t')), \phi_i \right\rangle_h dt' - \sigma \int_0^t \left\langle \sqrt{\tilde{\rho}_s(\cdot,t')} dW_s^{\mathcal{D}}(\cdot,t'), \nabla\phi_i(x) \right\rangle_h \\
&+ \sigma \int_0^t \left(\int_{\delta\tilde{D}} \left(\sqrt{\tilde{\rho}_s(x,t')} dW_s^{\mathcal{D}}(x,t') \cdot \hat{u}(x) \right) \phi_i(x)\, dx \right) + \sum_{r=1}^{N_R} \nu_s^r \int_0^t \left\langle \sqrt{a^r(\tilde{\rho}(\cdot,t'))} dW_r^{\mathcal{I}}(\cdot,t'), \phi_i \right\rangle_h \\
&\forall t \in [0,T] \text{ and for all test functions } \phi_i \in \tilde{V}, i = 0, \dots, n. \qquad (17)
\end{aligned}$$

To get the initial data of the discretization, we have to project the given $\rho_{s,0}(x)$ onto $\tilde{V}$, i.e.

$$\tilde{\rho}_{s,0}(x) = \sum_{j=0}^n \langle \rho_{s,0}, \phi_j\rangle \phi_j(x).$$

With $\{\tilde{\rho}_s(\cdot,t)\}_{t\in[0,T]}$ being a $\tilde{V}$-valued stochastic process, we can next expand a realization of $\{\tilde{\rho}_s(\cdot,t)\}_{t\in[0,T]}$ as a linear combination of the basis functions $\{\phi_j\}_{j=0}^n$ with time-dependent (and random) coefficients $\beta_{s,j}(t)$, i.e.

$$\tilde{\rho}_s(x,t) = \sum_{j=0}^n \beta_{s,j}(t)\phi_j(x). \qquad (18)$$

We define matrices

$$C := (C_{ij})_{i,j=0}^n = \left(\langle \phi_j, \phi_i\rangle_h\right)_{i,j=0}^n, \qquad (19)$$

$$A := (A_{ij})_{i,j=0}^n = \left(\frac{\sigma^2}{2} \langle \nabla\phi_j, \nabla\phi_i\rangle_h - \langle \nabla\cdot(\nabla V\phi_j), \phi_i\rangle_h \right)_{i,j=0}^n, \qquad (20)$$

the coefficient vector

$$\beta_s(t) := (\beta_{s,j}(t))_{j=0}^n, \qquad (21)$$

and the vector of the deterministic (non-linear) interaction term coupling the densities via $a^r(\tilde{\rho}(x,t))$

$$F_s(t) = (F_{s,i}(t))_{i=0}^n := \left(\sum_{r=1}^{N_r} \nu_s^r \langle a^r(\tilde{\rho}(\cdot,t)), \phi_i\rangle_h \right)_{i=0}^n. \qquad (22)$$

Inserting the expansion (18) into (17) and using the defined quantities (19) - (22), we finally arrive at

$$\sum_{j=0}^{n} C_{ij} d\beta_{s,j}(t) = -\sum_{j=0}^{n} A_{ij}\beta_{s,j}(t)\ dt + F_{s,i}(t)\ dt - \sigma \left\langle \sqrt{\tilde{\rho}_s(\cdot,t)} dW_s^{\mathcal{D}}(\cdot,t), \nabla\phi_i \right\rangle_h$$
$$+ \sigma \int_{\delta\tilde{D}} \left(\sqrt{\tilde{\rho}_s(x,t)} dW_s^{\mathcal{D}}(x,t) \cdot \hat{u}(x) \right) \phi_i(x)\ dx + \sum_{r=1}^{N_R} \nu_s^r \left\langle \sqrt{a^r(\tilde{\rho}(\cdot,t))} dW_r^{\mathcal{I}}(\cdot,t), \phi_i \right\rangle_h,$$
$$\forall t \in [0,T],\ \forall i = 0,\dots,n, \tag{23}$$

which is still understood as a time integral equation in the sense of (17).

3.2.2 Truncation of the Noise Expansion

By truncating the noise expansion (15) to M dimensions, we project the Cylindrical Wiener processes onto the finite-dimensional space spanned by $\{\chi_m\}_{m=1}^M$. The choice of the truncation threshold M remains an open question (e.g. [40, Theorem 10.41]). In our numerical experiments we will choose $M = n$.

The truncated expansion for the interaction noise reads

$$W_r^{\mathcal{I},M}(x,t) := \sum_{m=1}^{M} \chi_m(x) B_{r,m}^{\mathcal{I}}(t), \tag{24}$$

where $B_{r,m}^{\mathcal{I}}(t)$ denote i.i.d. Brownian motions in $\mathbb{R}$. Analogously for the diffusion noise, we replace $W_s^{\mathcal{D}}(x,t)$ by the truncated noise expansion[4]

$$W_s^{\mathcal{D},M}(x,t) := \sum_{m=1}^{M} \chi_m(x) B_{s,m}^{\mathcal{D}}(t), \tag{25}$$

where $B_{s,m}^{\mathcal{D}}(t) = (B_{s,m,l}^{\mathcal{D}}(t))_{l=1,\dots,d}$ denote i.i.d. Brownian motions in $\mathbb{R}^d$.

Then by defining the vectors

$$B_r^{\mathcal{I},M}(t) := (B_{r,m}^{\mathcal{I}}(t))_{m=1}^M$$
$$B_{s,l}^{\mathcal{D},M}(t) := \left(B_{s,m,l}^{\mathcal{D}}(t)\right)_{m=1}^M$$

and matrices

$$G_{s,l}^{\mathcal{D}}(t)_{im} := -\sigma \left\langle \sqrt{\tilde{\rho}_s(\cdot,t)}\chi_m, \frac{\partial\phi_i}{\partial x_l} \right\rangle_h + \sigma \int_{\delta\tilde{D}} \left(\sqrt{\tilde{\rho}_s(x,t)}\chi_m(x)\ \hat{u}_l(x) \right) \phi_i(x)\ dx \text{ for } l = 1,\dots,d \tag{26}$$

and

$$G_{s,r}^{\mathcal{I}}(t)_{im} := \nu_s^r \left\langle \sqrt{a^r(\tilde{\rho}(\cdot,t))}\chi_m, \phi_i \right\rangle_h, \text{ where } i = 0,\dots,n,\ m = 1,\dots,M, \tag{27}$$

our Galerkin approximation finally reads

$$C d\beta_s(t) = (-A\beta_s(t) + F_s(t))\ dt + \sum_{l=1}^{d} G_{s,l}^{\mathcal{D}}(t)\ dB_{s,l}^{\mathcal{D},M}(t) + \sum_{r=1}^{N_R} G_{s,r}^{\mathcal{I}}(t)\ dB_r^{\mathcal{I},M}(t). \tag{28}$$

Next, we will discretize this system of SDEs (28) in time using the (backward or semi-implicit) Euler-Maruyama method.

[4]The choice of the threshold M could in general be different for (24) and (25).

3.2.3 Time Discretization

The last step is to discretize in time, we divide the time interval $[0, T]$ into K intervals of sufficiently small size Δt. Denoting functions at time $t_k = k\Delta t$ by a subscript k, e.g. $\beta_s(t_k) = \beta_{s,k}$, the semi-implicit Euler-Maruyama time-discretization (implicit in the linear terms, explicit in the non-linear coupling term) of (28) is the recursion for $k = 0, \dots, K-1$

$$\beta_{s,k+1} = (C + A\Delta t)^{-1} \left(C\beta_{s,k} + F_{s,k}\Delta t + \sum_{l=1}^{d} G^{\mathcal{D}}_{s,l,k} \Delta B^{\mathcal{D}}_{s,l,k} + \sum_{r=1}^{N_R} G^{\mathcal{I}}_{s,r,k} \Delta B^{\mathcal{I}}_{r,k} \right). \tag{29}$$

The Brownian increments

$$\Delta B_k = \left(\int_{t_k}^{t_{k+1}} dB_m(t) \right)_{m=1}^{M} = (B_m(t_{k+1}) - B_m(t_k))_{m=1}^{M} = \left(\sqrt{\Delta t} \zeta_{m,k} \right)_{m=1}^{M}$$

have to be sampled for each time step t_k and for each $s = 1, \dots, N_T$, $l = 1, \dots, d$ and $r = 1, \dots, N_R$ by drawing i.i.d. $\zeta_{m,k} \sim \mathcal{N}(0, 1)$.

It is known that this time discretization converges globally [32] with convergence order $1/2$ for $\Delta t \to 0$.

Remark. One numerical problem is that the agent density can become negative in the simulations [36]. This is only due to the discretization and vanishes for $\Delta t \to 0$. When modeling the interactions between different densities and for a not too small time step Δt, it can happen that too much density is subtracted from one type. One possibility for tackling this problem in the implementation is to work with $\max\{0, \beta_{s,j,k}\}$ instead of $\beta_{s,j,k}$ and thereby to ensure its non-negativity.

4 Numerical Studies

Many models of real-world dynamics pose challenges regarding their simulation due to a complex model formulation. The agent-based model as introduced in Section 2.1 can be considered as the ground-truth model for a system of diffusing and interacting agents. However due to its high model complexity for large numbers of agents, simulations are often too expensive. The ABM is valid on all population scales but we expect its computational feasibility only on the smallest population scale. Reduced model descriptions are therefore needed, these reduced models should have a small approximation error as well as being computationally much more efficient. In Section 3.1, we presented a reduced model in terms of stochastic PDEs approximating the original ground-truth system with full spatial resolution and for large populations, whilst still including stochasticity.

In this section, we will illustrate both modeling approaches on a toy example of innovation spreading among humans that has real-world applications [8, 7, 44]. After studying each of the dynamics in some detail for a fixed number of agents in Section 4.1 and 4.2, we will in Section 4.3 compare the two modeling approaches for different population sizes regarding their computational cost and the approximation quality of the system of SPDEs to the ABM.

4.1 Illustrative Example: Modeling with Agents

We study $N = 3000$ agents diffusing with diffusion constant $\sigma = 0.25$ in the double well landscape $V(x) = (3.6(x-0.5)^2 - 0.1)^2$ on $D = [0, 1]$, see Figure 2. The suitability landscape V is characterized by two minima centered at $x = \frac{1}{3}$ and $x = \frac{2}{3}$, corresponding to the most suitable areas for agents and a barrier between the two wells. Thus the agents will spend most of their time near the centers of the two wells while rarely transitioning between them.

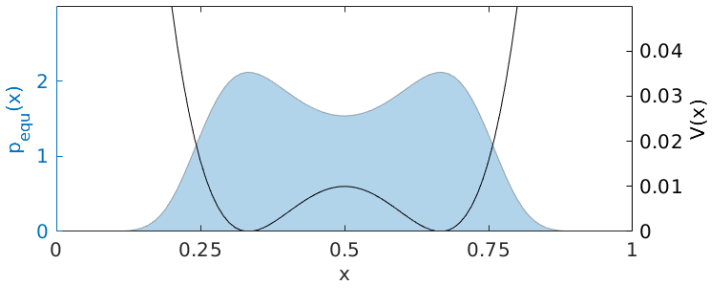

Figure 2: Suitability landscape V and the corresponding unique equilibrium distribution for the position of one agent $p_{\text{equ}}(x) = Z^{-1} \exp\left(-2\sigma^{-2}V(x)\right)$, the distribution is normalized by Z.

On top of the position dynamics, agents are interacting whenever they are close-by. We consider the spreading of an innovation given by the rule $R_1 : T_1 + T_2 \to 2\ T_2$ at fixed influence rate $\gamma^1_{\text{ABM}} = 0.5$ whenever two agents of type T_1 (non-adopter of the innovation) and T_2 (adopter of the innovation) are within radius $d_{\text{int}} = 0.001$ of each other.

We will describe the dynamics by the coupled ABM equations (7) and simulate approximate realizations of the process with step size $\Delta t = 0.001$ as explained in Section 2.2. We assume that at $t = 0$, the positions of the initially 2800 agents of type T_1 are normally distributed with mean 0.5 and standard deviation 0.2. Similarly, for the 200 agents of type T_2, we draw the initial positions from the normal distribution $\mathcal{N}(0.7, 0.05)$.
Some snapshots of one simulation of the spreading process are given in Figure 3.

We observe the following dynamics: At time $t = 0$, the innovation starts spreading in the well centered at $x = \frac{2}{3}$. The agents quickly distribute near the attractive centers of the two wells. It takes some time until the innovation reaches the other well centered at $x = \frac{1}{3}$. But as soon as an adopter agent crosses the barrier for the first time, the innovation quickly gets adopted by all agents in the other well. At the final time $t = 2$, all agents are of type T_2 and distributed according to the equilibrium distribution of the landscape V (see Figure 2).

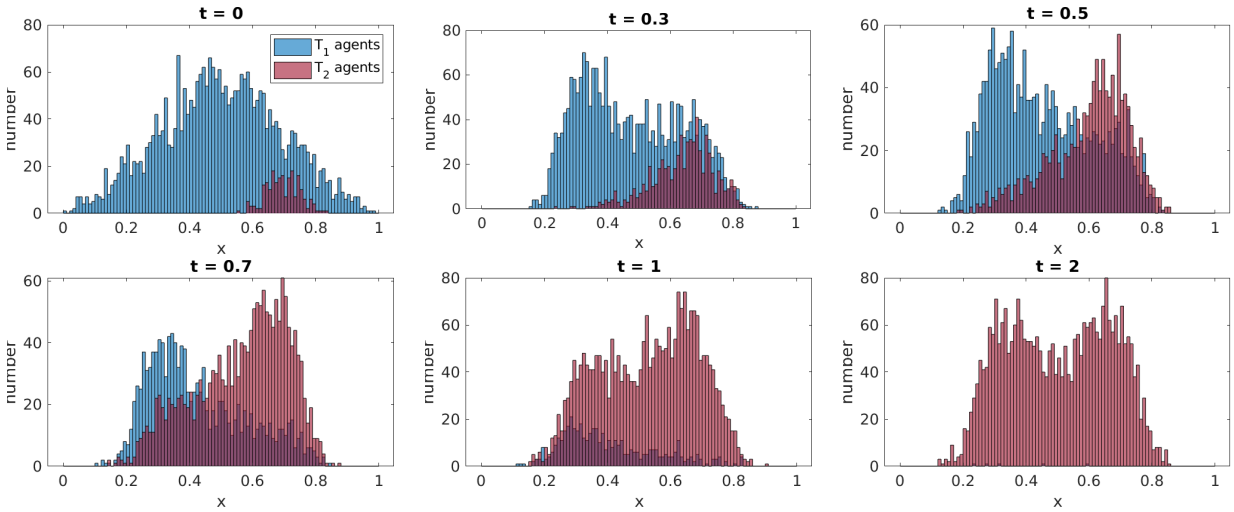

Figure 3: A single realization of the spreading process in a double well landscape on $D = [0, 1]$ with 3000 agents and modeled by the ABM. The empirical density of the positions of T_1 agents at time t is given by the blue histogram while the positions of the type T_2 agents are plotted using the red histogram.

4.2 Illustrative Example: Modeling with Agent Densities

As in the previous section, we consider two types of agents in a double well landscape that are spreading an innovation. But this time, we will model the dynamics using the system of SPDEs that evolves the two agent densities $\rho_1(x,t)$ (density of non-adopters) and $\rho_2(x,t)$ (density of adopters).

To get the initial conditions, two approaches are possible. Either we know the initial densities, or in the case that the positions and types of the N agents at time $t = 0$ are given, we can construct the initial densities $\rho_{s,0}(x)$ by summing unit masses (e.g. Dirac Deltas, narrow Gaussian functions, normalized hat functions) placed at the position of each agent of type T_s. In this example, we will take the first approach by using (similar as in the previous model setting) that the agent positions are normally distributed, i.e. $\rho_{1,0}(x)$ and $\rho_{2,0}(x)$ are Gaussian functions integrating to the number of agents of each type ($N_1 = 2800$ and $N_2 = 200$ respectively) at time $t = 0$.

Most parameter values of the SPDE model can be chosen equally to the ABM. It is only the micro-scale spreading rate γ^r_{ABM} in combination with the interaction radius d_{int} which has to be converted into an effective spreading rate γ^r_{SPDE} on the meso-scale. In general, this is still an open problem [15, 17]. To derive the effective meso-scale rate for type T_s agents at $x \in D$ due to rule R_r, we have to take the neighbouring agents of type $T_{s''}$ inside a closed ball $B_{\text{int}}(x)$ of radius d_{int} into account, s.t. the transition rate function (13) becomes

$$a^r(\rho(x,t)) = \rho_s(x,t)\gamma^r_{\text{ABM}} \int_{B_{\text{int}}(x)} \rho_{s''}(x',t)dx'.$$

Assuming that the agent densities are approximately constant inside $B_{\text{int}}(x)$ of volume V_{int}, we arrive at

$$a^r(\rho(x,t)) \approx V_{\text{int}}\gamma^r_{\text{ABM}}\rho_s(x,t)\rho_{s''}(x,t). \tag{30}$$

Thus we converted the meso-scale rate by $\gamma^r_{\text{SPDE}} = V_{\text{int}}\gamma^r_{\text{ABM}}$ [17]. In 1D, this simply reduces to $\gamma^r_{\text{SPDE}} = 2\ d_{\text{int}}\gamma^r_{\text{ABM}}$.

Given the model setting, we can turn to the specification of the discretization. Numerically sampling trajectories of the SPDE system can be done by iteratively solving (29) in parallel for both agent types $s = 1, 2$.
For the space discretization, we split the domain $D = [0,1]$ into equidistant grid cells of size $h = \frac{1}{n}$ (s.t. $\tilde{D}(h) = D$), supporting the hat functions $\phi_i(x)$, $i = 0, \dots, n$, defined as

$$\phi_i(x) := \begin{cases} 0 & x < x_{i-1} \text{ or } x \geq x_{i+1} \\ \frac{x - x_{i-1}}{h} & x_{i-1} \leq x < x_i \\ 1 - \frac{x - x_i}{h} & x_i \leq x < x_{i+1}, \end{cases}$$

where $x_i = ih$. The hat functions are spanning our Finite Element space $\tilde{V}$.
For the expansion of the cylindrical Wiener process, we choose the trigonometric system as an orthonormal basis for $L^2(D)$.
The matrices (19), (20), (26), (27) can be assembled by analytical or numerical integration, or by defining a reference element and transforming from any grid cell to the reference grid cell in order to do the computations on the reference cell before transforming back [39]. Since each hat function is mostly zero throughout $\tilde{D}$, the resulting matrices will be sparse.

Snapshots of one realization of the agent dynamics are shown in Figure 4, where as discretization parameters we choose $n = M = 256$ and time steps of size $\Delta t = 0.001$. We plot the time evolution of the densities $\rho_1(x,t)$ and $\rho_2(x,t)$.

The emerging dynamics agree with the ABM dynamics in Figure 3. Again the agent densities are clustered around the two wells. The spreading of the innovation among agents inside the same well is fast, but the spreading of the innovation from one well to another takes much longer. We observe that the stochasticity inherent in the model is still visible on the global scale, the agent densities are seemingly noisy. The noisiness as well as the overall dynamics resemble the snapshots of the dynamics when modeled by the ABM.
In the next part, we will investigate this question further and study a larger sample of simulations as well as different population sizes N.

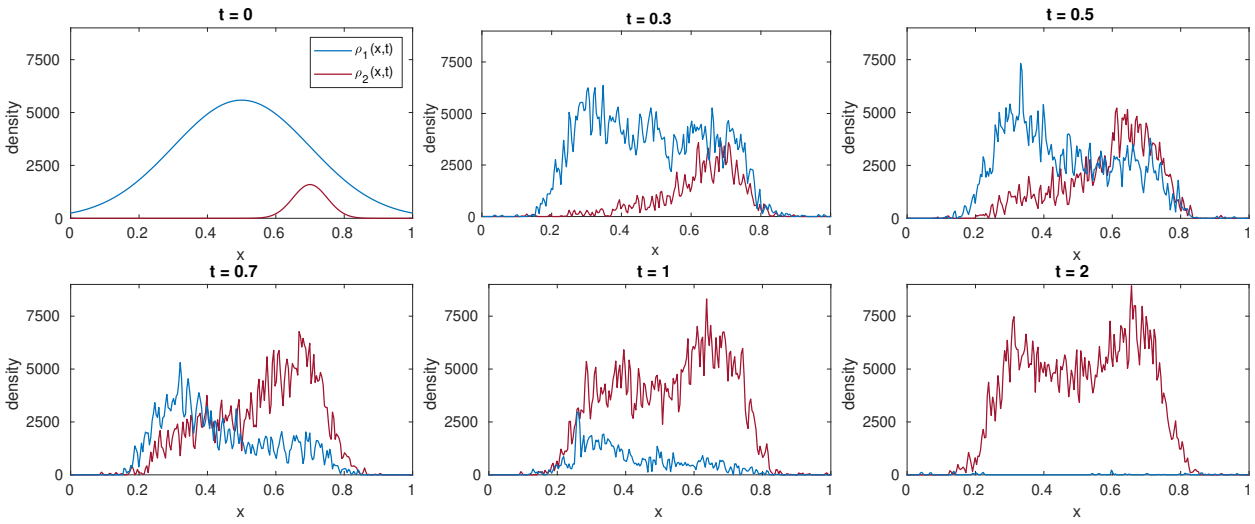

Figure 4: Realization of a spreading process in a double well landscape on $D = [0, 1]$ with 3000 agents (SPDE approach). We plot the density of non-adopters $\rho_1(x, t)$ (in blue) and the density of adopters $\rho_2(x, t)$ (in red) at a few time instances.

4.3 Comparison of the Models

Considering the ABM as the ground-truth model, we compare the innovation spreading dynamics (as introduced in the previous Sections 4.1 and 4.2) for different population sizes using the ABM and the reduced SPDE model. In particular, we are studying how the agent-based and SPDE model compare in computation time and at which agent numbers N the SPDE model starts to be a good approximation to the ABM.

We simulate both models for varying population sizes $N \in [300, 5000]$. For each N, we consider an ensemble of `sim` = 5000 realizations in order to compute meaningful ensemble averages. The simulation schemes are implemented in Matlab and run on a computer with an Opteron 8384 CPU.

The Computational Effort: For both models and varying N, we fix the step size in time to $\Delta t = 0.01$ and measure the time it takes to simulate one time step. Since both simulation approaches make use of an Euler-Maruyama time discretization, comparing the effort per time step is sensible. But space is treated differently. In the ABM, we use an Euler-Maruyama discretization for the position dynamics of each agent, whereas in the SPDE approach, we use the scheme for each hat function. Moreover, for the simulation of the ABM, we have to compute pair-wise distances between agents, which becomes very expensive for increasing agent numbers N. Thus we expect the computational effort for the ABM to depend on the number of agents, whereas for the SPDE model it should be independent of N and thus constant for increasing N.

Approximation Quality: We compute observables of the simulated dynamics for both models and

increasing agent numbers. Based on these measured observables, we can compare how well they agree and deduce the approximation quality of the SPDE description to the ABM[5]. Possible observables are e.g. the time it takes until the agent system has reached a certain state for the first time or the state of the system at a fixed time point. Here, we study innovation spreading dynamics in a double well landscape with the parameters chosen as in Sections 4.1, 4.2. The observables we consider are (i) the time until 90% of agents are of type T_2, and (ii) the spatial distribution of type T_s ($s = 1, 2$) agents at a fixed model time point, which we choose to be the mean of the first time that 90 % of agents in the ABM are of type T_2.

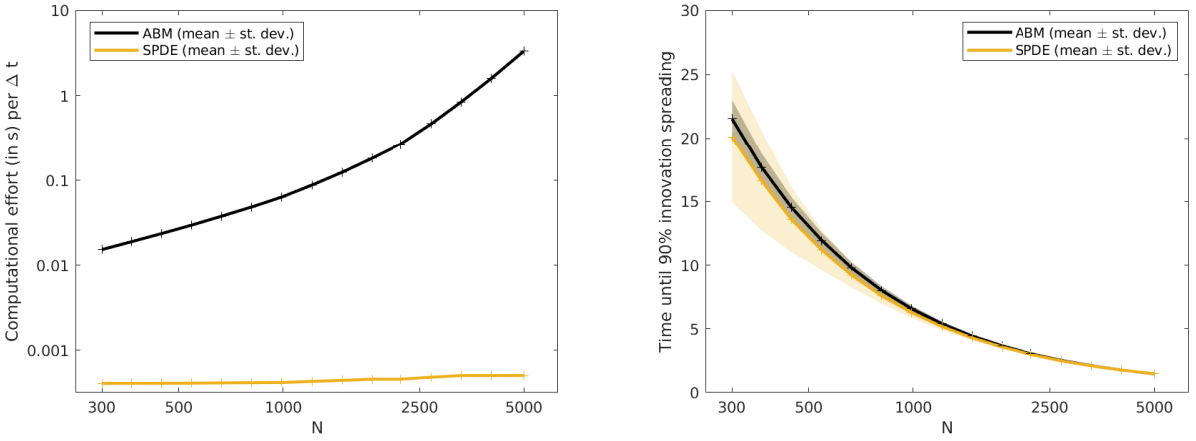

(a) Computational effort of both models.

(b) The first time that 90% of agents are adopters.

Figure 5: The computational effort and the approximation quality of the SPDE model to the ABM, where the mean and standard deviation are taken for an ensemble of `sim`=5000 realizations.

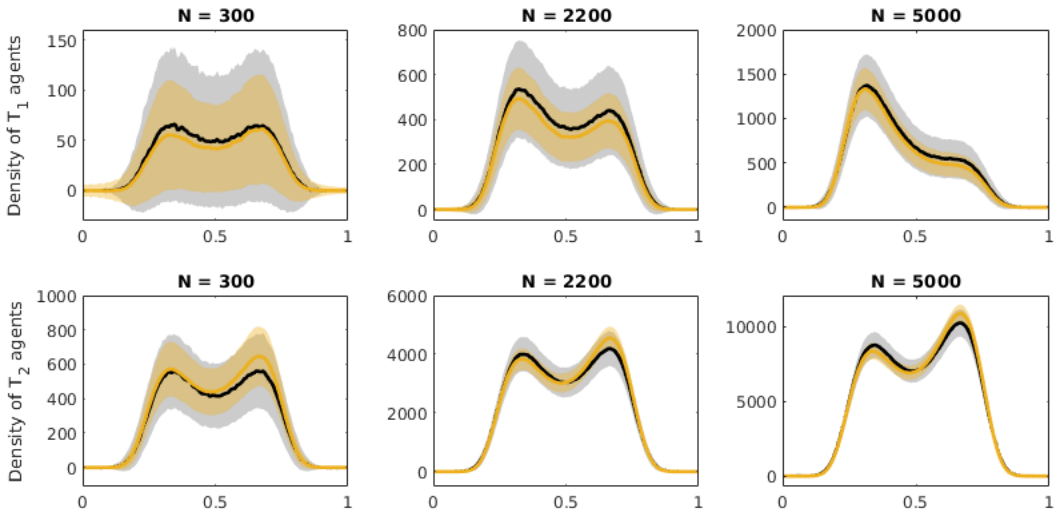

Figure 6: Spatial distribution on $[0, 1]$ of the number densities for a fixed time point, here taken as the mean first time of 90% adopters in the ABM as given by the black curve in Figure 5b. The outcome (mean and standard deviation) of the ABM is shown in black, the outcome of the SPDE model is depicted in yellow.

In the following we come to a discussion of the results. The results of the computational complex-

[5]Computing these observables we also make numerical and statistical errors.

ity studies are shown in Figure 5a. As expected, the computational effort for the ABM increases strongly, more precisely exponentially, with the number of agents, whereas the effort for the simulation of the density-based model remains cheap. The cost of simulating realizations of the SPDE is independent of N and several magnitudes below the cost of simulating the ABM.

Further, we compared observables of the density-based model with observables of the ABM in order to study the approximation quality, see Figures 5b and 6.
First of all, we remark that for increasing numbers of agents, the stochasticity in both models decreases as can be seen from the reducing standard deviation. The more agents in the ABM, the less the individual behaviour sticks out (due to the law of large numbers). For the SPDE model this was also expected (see the comment in Section 3.1.3), since the noise scaling of the SPDE is such that the noise dominates for small population sizes and has less influence for large population sizes.
Next for systems of very few agents (in our example around $N < 1000$), both observables agree roughly in mean between the two models. But for observable (i), the standard deviation of the SPDE model is much larger than the one of the ABM, whereas for observable (ii), it is the other way around, the noisiness of the ABM is larger than the one of the SPDE model.
For systems with a larger number of agents $N > 1000$, the global observable (i) in Figure 5b agrees well in mean and standard deviation, even though we notice that the spatial observable in Figure 6 indicates that the interactions in the SPDE take place slightly faster than the interactions in the ABM. Two points can explain this: First, replacing the Poisson process in the ABM by a Gaussian process in the SPDE model is only a valid approximation for large agent numbers in each grid cell. This issue was already mentioned in [4] and commented upon above in Remark 3.1.2. In [36] it is proposed to use Poisson noise in each grid cell after spatial discretization. However, we stick to the approximation by a normal distribution, since the approach in [36] is rather ad-hoc and cannot be extended to the continuous SPDE. Second, we converted the interaction rates in (30) by assuming that the density of agents is approximately constant inside a ball of radius d_{int}, but the densities are very noisy and rough and thus not at all constant inside small neighbourhoods.
Whether these two explanations might be valid or not is largely unclear, since a rigorous approach to understanding the joint convergence of the different models in the limit of large population, or in similar limits, is still missing and therefore, there also is a lack of understanding regarding the source of approximation errors.

5 Conclusion and Future Outlook

ABMs are the most natural approach to construct models for real-world systems containing discrete interacting entities such as humans, since one can simply model the actions of each individual. Based on [8, 7], we have described a general agent-based model that is formulated in terms of coupled diffusion and Markov jump processes for each agent.
Some further research regarding the construction of the ABM could be directed at the following questions:

- Is it reasonable to model human or agent mobility by Brownian motion with drift? One could also model the diffusion of agents on an infrastructure network or by a different stochastic process [3].
- Can we extend the ABM to include feedback loops, such that e.g. the type changes also influence the position dynamics?
- How can we quantify and analyse the resulting dynamics, e.g. by making use of transition path theory [16, 43]?

Simulating agent-based models for real-world dynamics quickly becomes costly due to an explosion in the computational complexity for increasing agent numbers and the need for repeated simulations due to its stochastic description. For instance, when modeling the spreading of innovations in ancient times such as in [8, 7], many Monte-Carlo simulation are required to capture the full spectrum of the diverse dynamics. But this becomes computationally very expensive. A thorough sensitivity analysis of the parameters demands many simulations for each parameter set and is as such not tractable.
Based on an extension of the Dean-Kawasaki model [36, 11, 34, 4, 30], we therefore considered a meso-scale approximation to the ABM for systems of many agents. The reduced model is given by a system of coupled stochastic PDEs propagating agent densities for the different agent types.
For both models, the ABM and the reduced density-based model, we constructed and explained simulation schemes. The Finite Element discretization of the system of SPDEs serves as an interpretation and regularization of the ill-defined SPDE for which solutions not necessarily exist [18, 9, 38].
There are however several questions that still remain unanswered and should be investigated further:

- The notion of the solution to the SPDE and its existence and uniqueness is still unclear due to several mathematical difficulties [9, 38, 18].
- Can we find quantitative statements for the approximation and discretization quality?
- Numerical experiments for higher spatial dimensions and more complex domains as well as studies on the applicability to real-world systems containing humans need to be investigated further.

Finally, we compared the simulation effort and studied the approximation quality of the reduced density-based model to the ABM computationally on a toy example of innovation spreading. From these computational experiments we can conclude the following. For systems of few agents, the ABM is not too costly. We consider the ABM as the ground-truth model and thus as the most accurate description of the agent system. The dynamics have to be described in terms of individual agents, since there are only very few.
But for systems of many agents, we can instead use the approximation by the SPDE to study the agent system dynamics much more efficiently. In the case of our toy example, this approximation is reasonably accurate in mean and standard deviation already for systems of 1000 agents. Thus, the presented reduced model is a very promising tool for modeling and especially simulating real-world systems with large agent populations. The SPDE model offers the possibility to carry out a more thorough model analysis such as parameter studies and inference, or model control, whilst staying numerically tractable.

Acknowledgments The authors thank Changho Kim for an insightful discussion on the Dean-Kawasaki equation with added reactions. The authors received funding by the Deutsche Forschungsgemeinschaft (DFG, German Research Foundation) under Germany's Excellence Strategy – The Berlin Mathematics Research Center MATH+ (EXC-2046/1, project ID: 390685689) and through grant CRC 1114.

References

[1] Peter Ashwin, Sebastian Wieczorek, Renato Vitolo, and Peter Cox. Tipping points in open systems: bifurcation, noise-induced and rate-dependent examples in the climate system. *Philosophical Transactions of the Royal Society A: Mathematical, Physical and Engineering Sciences*, 370(1962):1166–1184, 2012.

[2] Steven C Bankes. Agent-based modeling: A revolution? *Proceedings of the National Academy of Sciences*, 99(suppl 3):7199–7200, 2002.

[3] Hugo Barbosa, Marc Barthelemy, Gourab Ghoshal, Charlotte R James, Maxime Lenormand, Thomas Louail, Ronaldo Menezes, José J Ramasco, Filippo Simini, and Marcello Tomasini. Human mobility: Models and applications. *Physics Reports*, 734:1–74, 2018.

[4] Amit Kumar Bhattacharjee, Kaushik Balakrishnan, Alejandro L Garcia, John B Bell, and Aleksandar Donev. Fluctuating hydrodynamics of multi-species reactive mixtures. *The Journal of chemical physics*, 142(22):224107, 2015.

[5] Eric Bonabeau. Agent-based modeling: Methods and techniques for simulating human systems. *Proceedings of the national academy of sciences*, 99(suppl 3):7280–7287, 2002.

[6] Dirk Brockmann and Dirk Helbing. The hidden geometry of complex, network-driven contagion phenomena. *Science*, 342(6164):1337–1342, 2013.

[7] Nataša Conrad, Luzie Helfmann, Johannes Zonker, Stefanie Winkelmann, and Christof Schütte. Human mobility and innovation spreading in ancient times: A stochastic agent-based simulation approach. *EPJ Data Science*, 7(1):24, 2018.

[8] Nataša Djurdjevac Conrad, Daniel Furstenau, Ana Grabundžija, Luzie Helfmann, Martin Park, Wolfram Schier, Brigitta Schütt, Christof Schütte, Marcus Weber, Niklas Wulkow, and Johannes Zonker. Mathematical modeling of the spreading of innovations in the ancient world. *eTopoi. Journal for Ancient Studies*, 7, 2018.

[9] Federico Cornalba, Tony Shardlow, and Johannes Zimmer. A regularized dean–kawasaki model: Derivation and analysis. *SIAM Journal on Mathematical Analysis*, 51(2):1137–1187, 2019.

[10] Giuseppe Da Prato and Jerzy Zabczyk. *Stochastic equations in infinite dimensions*. Cambridge university press, 2014.

[11] David S Dean. Langevin equation for the density of a system of interacting langevin processes. *Journal of Physics A: Mathematical and General*, 29(24):L613, 1996.

[12] Steven Delong, Boyce E Griffith, Eric Vanden-Eijnden, and Aleksandar Donev. Temporal integrators for fluctuating hydrodynamics. *Physical Review E*, 87(3):033302, 2013.

[13] Masao Doi. Stochastic theory of diffusion-controlled reaction. *Journal of Physics A: Mathematical and General*, 9(9):1479, 1976.

[14] Aleksandar Donev, Eric Vanden-Eijnden, Alejandro Garcia, John Bell, et al. On the accuracy of finite-volume schemes for fluctuating hydrodynamics. *Communications in Applied Mathematics and Computational Science*, 5(2):149–197, 2010.

[15] Aleksandar Donev, Chiao-Yu Yang, and Changho Kim. Efficient reactive brownian dynamics. *The Journal of Chemical Physics*, 148(3):034103, 2018.

[16] Weinan E and Eric Vanden-Eijnden. Towards a theory of transition paths. *Journal of statistical physics*, 123(3):503, 2006.

[17] Radek Erban and S Jonathan Chapman. Stochastic modelling of reaction–diffusion processes: algorithms for bimolecular reactions. *Physical biology*, 6(4):046001, 2009.

[18] Benjamin Fehrman and Benjamin Gess. Well-posedness of nonlinear diffusion equations with nonlinear, conservative noise. *Archive for Rational Mechanics and Analysis*, pages 1–74, 2019.

[19] Peter G Fennell, Sergey Melnik, and James P Gleeson. Limitations of discrete-time approaches to continuous-time contagion dynamics. *Physical Review E*, 94(5):052125, 2016.

[20] Ronald Aylmer Fisher. The wave of advance of advantageous genes. *Annals of eugenics*, 7(4):355–369, 1937.

[21] Nigel Gilbert and Steven Bankes. Platforms and methods for agent-based modeling. *Proceedings of the National Academy of Sciences*, 99(suppl 3):7197–7198, 2002.

[22] Daniel T Gillespie. The chemical langevin equation. *The Journal of Chemical Physics*, 113(1):297–306, 2000.

[23] Tobias Grafke, Michael E Cates, and Eric Vanden-Eijnden. Spatiotemporal self-organization of fluctuating bacterial colonies. *Physical review letters*, 119(18):188003, 2017.

[24] Shawn Graham. Networks, agent-based models and the antonine itineraries: implications for roman archaeology. *Journal of Mediterranean Archaeology*, 19(1):45–64, 2006.

[25] Cameron S Griffith, Byron L Long, and Jeanne M Sept. Hominids: An agent-based spatial simulation model to evaluate behavioral patterns of early pleistocene hominids. *Ecological Modelling*, 221(5):738–760, 2010.

[26] Volker Grimm, Uta Berger, Donald L DeAngelis, J Gary Polhill, Jarl Giske, and Steven F Railsback. The odd protocol: a review and first update. *Ecological modelling*, 221(23):2760–2768, 2010.

[27] Volker Grimm and Steven F Railsback. *Individual-based modeling and ecology*, volume 8. Princeton university press, 2013.

[28] Volker Grimm, Eloy Revilla, Uta Berger, Florian Jeltsch, Wolf M Mooij, Steven F Railsback, Hans-Hermann Thulke, Jacob Weiner, Thorsten Wiegand, and Donald L DeAngelis. Pattern-oriented modeling of agent-based complex systems: lessons from ecology. *science*, 310(5750):987–991, 2005.

[29] Dirk Helbing. Agent-based modeling, 2012.

[30] Luzie Helfmann. Stochastic modeling of interacting agent systems. *Master's Thesis, Freie Universität Berlin*, 2018.

[31] Desmond J Higham. An algorithmic introduction to numerical simulation of stochastic differential equations. *SIAM review*, 43(3):525–546, 2001.

[32] D.J. Higham, X. Mao, and A.M Stuart. Strong convergence of Euler-type methods for nonlinear stochastic differential equations. *SIAM J. Numer. Anal.*, 40(3):1041–1063, 2002.

[33] Petter Holme and Mark EJ Newman. Nonequilibrium phase transition in the coevolution of networks and opinions. *Physical Review E*, 74(5):056108, 2006.

[34] Kyozi Kawasaki. New method in non-equilibrium statistical mechanics of cooperative systems. In *Synergetics*, pages 35–44. Springer, 1973.

[35] William O Kermack and Anderson G McKendrick. A contribution to the mathematical theory of epidemics. In *Proceedings of the Royal Society of London A: mathematical, physical and engineering sciences*, volume 115, pages 700–721. The Royal Society, 1927.

[36] Changho Kim, Andy Nonaka, John B Bell, Alejandro L Garcia, and Aleksandar Donev. Stochastic simulation of reaction-diffusion systems: A fluctuating-hydrodynamics approach. *The Journal of chemical physics*, 146(12):124110, 2017.

[37] Peter E Kloeden and Eckhard Platen. *Numerical Solution of Stochastic Differential Equations*. Springer, 1992.

[38] Vitalii Konarovskyi, Tobias Lehmann, and Max-K von Renesse. Dean-kawasaki dynamics: ill-posedness vs. triviality. *Electronic Communications in Probability*, 24, 2019.

[39] Stig Larsson and Vidar Thomée. *Partial differential equations with numerical methods*, volume 45. Springer Science & Business Media, 2008.

[40] Gabriel J Lord, Catherine E Powell, and Tony Shardlow. *An introduction to computational stochastic PDEs*, volume 50. Cambridge University Press, 2014.

[41] Michael W Macy and Robert Willer. From factors to actors: computational sociology and agent-based modeling. *Annual review of sociology*, 28(1):143–166, 2002.

[42] Xuerong Mao. *Stochastic Differential Equations and Applications*. Woodhead Publishing, second edition, 2008.

[43] Philipp Metzner, Christof Schütte, and Eric Vanden-Eijnden. Transition path theory for markov jump processes. *Multiscale Modeling & Simulation*, 7(3):1192–1219, 2009.

[44] Martin Park, Nataša Djurdjevac Conrad, Ana Grabundzija, Luzie Helfmann, Emmanuele Russo, Marcus Weber, Johannes Zonker, Wolfram Schier, Christof Schütte, and Brigitta Schütt. Modeling the spread of the wool-bearing sheep from south-west asia into europe – an agent-based approach. Submitted.

[45] Romualdo Pastor-Satorras, Claudio Castellano, Piet Van Mieghem, and Alessandro Vespignani. Epidemic processes in complex networks. *Reviews of modern physics*, 87(3):925, 2015.

[46] John E Pearson. Complex patterns in a simple system. *Science*, 261(5118):189–192, 1993.

[47] Marten Scheffer, Steve Carpenter, Jonathan A Foley, Carl Folke, and Brian Walker. Catastrophic shifts in ecosystems. *Nature*, 413(6856):591, 2001.

[48] Frank Schweitzer. Modelling migration and economic agglomeration with active brownian particles, 2002.

[49] Christian L Vestergaard and Mathieu Génois. Temporal gillespie algorithm: Fast simulation of contagion processes on time-varying networks. *PLOS computational biology*, 11(10):e1004579, 2015.